Preprints.org

Review

Not peer-reviewed version

Biomolecular Condensates of Interferon-Inducible Human and Murine Antiviral Mx Proteins

Pravin B. Sehgal *

Posted Date: 26 September 2024

doi: 10.20944/preprints202409.1952.v1

Keywords: interferon; myxovirus resistance proteins; MxA and Mx1; biomolecular condensates; metasability; rapidly reversible osmosensing; saliva-like hypotonicity; regulatory volume decrease (RVD); WNK-SPAK/OSR1 kinase pathway; oral antiviral defense

Preprints.org is a free multidiscipline platform providing preprint service that is dedicated to making early versions of research outputs permanently available and citable. Preprints posted at Preprints.org appear in Web of Science, Crossref, Google Scholar, Scilit, Europe PMC.

Copyright: This is an open access article distributed under the Creative Commons Attribution License which permits unrestricted use, distribution, and reproduction in any medium, provided the original work is properly cited.

Preprints.org (www.preprints.org) | NOT PEER-REVIEWED | Posted: 26 September 2024 doi:10.20944/preprints202409.1952.v

Disclaimer/Publisher's Note: The statements, opinions, and data contained in all publications are solely those of the individual author(s) and contributor(s) and not of MDPI and/or the editor(s). MDPI and/or the editor(s) disclaim responsibility for any injury to people or property resulting from any ideas, methods, instructions, or products referred to in the content.

Review

Biomolecular Condensates of Interferon-Inducible Human and Murine Antiviral Mx Proteins

Pravin B. Sehgal [1,2]

[1] Department of Cell Biology and Anatomy, New York Medical College, Valhalla, New York 10595USA; pravin_sehgal@nymc.edu

[2] Department of Medicine, New York Medical College, Valhalla, New York 10595, USA

Abstract: Type I (IFN-α/β) and Type III (IFN-λ) interferon-inducible myxovirus resistance (Mx) proteins have long been recognized to inhibit a broad spectrum of RNA- and DNA-containing viruses (1-5). Mx proteins are dynamin-family GTPases of size 60-70 kDa (1-3) with different subcellular localization and antiviral activities. In the last 5 years there has been a paradigm shift in our understanding of the structures formed by human and murine Mx proteins in the cytoplasm and nucleus. We now recognize that the major *human* MxA protein forms structures in the cytoplasm and the major *murine* Mx1 forms structure in the nucleus which comprise liquid-liquid phase separated (LLPS) biomolecular condensates [membraneless organelles (MLOs)] with a gel-like internal consistency. The second human Mx protein, MxB, which had been previously observed to associate with the cytoplasmic face of nuclear pores, was also recently confirmed to represent cytoplasmic biomolecular condensates. Our overall focus now is to understand the formation, dynamics and antiviral function of biomolecular condensates of different Mx proteins in the cytoplasm and nucleus in cells of different species. We highlight the metastability and rapidly reversible hypotonicity sensing properties of MxA condensates in human cells, especially as applicable to environmental stress inflicted on the oral mucosa.

Keywords: interferon; myxovirus resistance proteins; MxA and Mx1; biomolecular condensates; metasability; rapidly reversible osmosensing; saliva-like hypotonicity; regulatory volume decrease (RVD); WNK-SPAK/OSR1 kinase pathway; oral antiviral defense

1. Introduction

Originally identified for their role in antiviral resistance of mice to inhaled challenge with influenza A myxovirus (FLUAV), the Type I (IFN-α/β) and Type III (IFN-λ) interferon-inducible "myxovirus" resistance (Mx) proteins are now recognized to inhibit a broad spectrum of RNA- and DNA-containing viruses [1–8]. Mx proteins are dynamin-family GTPases of size 60-70 kDa with different subcellular localization and antiviral activities (Table 1, Figure 1)[1–3]. Despite extensive investigations, the molecular mechanisms of the Mx antiviral effects are incompletely understood [1–8]. The GTPase activity is necessary for inhibition of most, but not all, viruses by Mx proteins [1–3]. While in 2002 Koch and colleagues [9] already reported that human MxA formed structures in the cytoplasm that did not match any membrane-bound organellar markers and also lacked a surrounding membrane (as judged by thin-section electron microscopy), numerous investigators since 2002 have followed the lead of Accola et al [10] and Stertz et al [11] and state that human MxA associated with the endoplasmic reticulum (ER)(reviewed in [12–14]). In the last 5 years we have replicated the experimental observation of Stertz et al reported in 2006 [11] of the occurrence of HA-MxA in a cytoplasmic meshwork in human Huh7 hepatoma cells, but have provided data to re-interpret that meshwork as the association of HA-MxA biomolecular condensates with a novel giantin-based intermediate filament meshwork in Huh7 cells, not so much with the ER [12,13]. Moreover, we confirmed the observations reported by Koch et al in 2002 [9]that human MxA structures in the cytoplasm of virus-infected cells were membraneless using correlated light and

© 2024 by the author(s). Distributed under a Creative Commons CC BY license.

Preprints.org (www.preprints.org) | NOT PEER-REVIEWED | Posted: 26 September 2024 doi:10.20944/preprints202409.1952.v

electron microscopy (CLEM) methods [12,13]. These data led to the paradigm shift that Mx proteins mainly formed liquid-liquid phase-separated (LLPS) membraneless metastable biomolecular condensates in the intact cell cytoplasm and nucleus (Table 1, Figure 1)[12–15]. Moreover, human MxA structures in the cytoplasm and murine Mx1 structure in the nucleus comprised LLPS-driven membraneless organelles (MLOs) with a gel-like internal consistency as determined using fluorescence recovery after photobleaching (FRAP) methods [12]. The second human Mx protein, MxB, which had been previously observed to form structures associated with the cytoplasmic face of nuclear pores [16,17], was also confirmed very recently by Moschonas et al to represent cytoplasmic membraneless biomolecular condensates [18]. Our overall focus now is to understand the formation, dynamics and antiviral function of biomolecular condensates of human and murine Mx proteins. In this review we highlight the amazing metastability of MxA condensates in human cancer cells, especially the rapidly reversible osmosensing properties, and point to the many open questions.

Table 1. Properties of different human and murine Mx proteins.

Protein	Cellular localization	Illustrative Antiviral activity*	References
Human MxA	cytoplasmic condensates with some tethered to intermediate filaments	vs both FLUAV and VSV	[9,12–15]
Human MxB (full length)	cytoplasmic face of nuclear pores, Cytoplasmic condensates	vs HIV; not vs FLUAV nor VSV	[16–18,31] [18]
Murine Mx1	nuclear condensates	vs FLUAV; not VSV	[32]
	cytoplasmic intermediate filaments and condensates	vs VSV	[32]
Murine Mx2	cytoplasmic structures,	vs VSV; not FLUAV	[33]

*See reviews [3,4,7] for additional literature. Adapted from ref. [32].

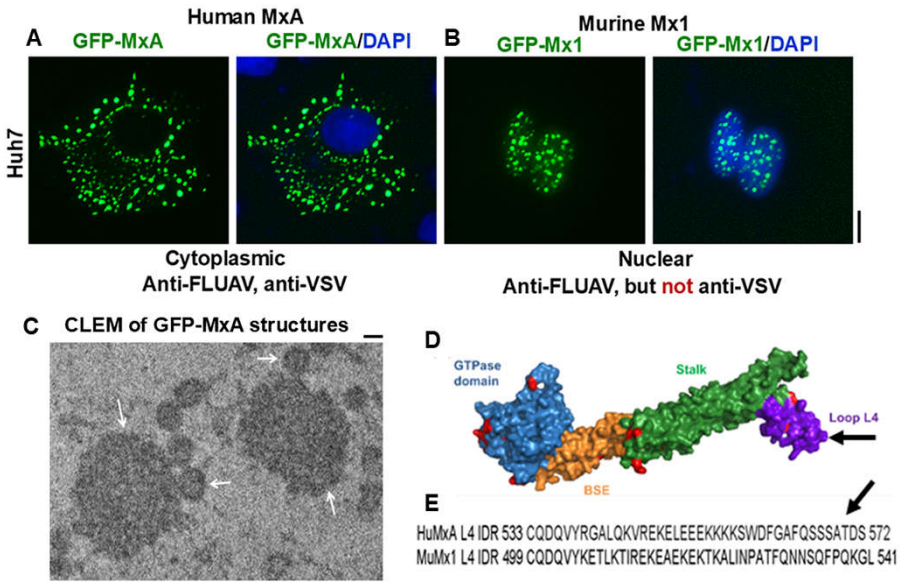

Figure 1. (A) and **(B)** Human hepatoma Huh7 cells were imaged two days after transient transfection with expression vectors for human GFP-MxA or murine GFP-Mx1 respectively. Scale bar = 10 μm. **(C)** Thin-section electron micrograph of GFP-MxA structures (white arrows) identified by correlated light

Preprints.org (www.preprints.org) | NOT PEER-REVIEWED | Posted: 26 September 2024 doi:10.20944/preprints202409.1952.v

and electron microscopy (CLEM). Scale bar = 200 nm. (D) structure of MxA; arrow points to loop L4. (E) Sequence of loop L4 in HuMxA (arrow) and corresponding sequence in MuMx1; region represents an intrinsically disordered domain. Adapted from refs [12,32].

By way of background, MLOs in the cytoplasm and nucleus in the form of liquid-liquid phase-separated (LLPS) biomolecular condensates are now increasingly viewed as critical regulators of diverse cellular and biochemical functions [15,19–23]. Cytoplasmic and nuclear phase-separated biomolecular condensates have emerged as providing scaffolding for diverse subcellular functions including but not limited to epigenetic regulation, DNA repair, transcription, RNA processing, mRNA translation, stress responses including to hypoxia, tonicity, temperature, pH, and normal and aberrant signaling from the plasma membrane to the cell interior. More recently condensate droplet formation by fusion oncoproteins leading to aberrant prooncogenic signaling, involvement of condensates in mechanisms of innate and adaptive immunity, cytokine signaling, viral replication and antiviral mechanism, and condensate targeting by cancer therapeutic agents have been highlighted in numerous investigations [14,24–26]. Moreover, there is increasing understanding of the involvement of such LLPS condensates in mechanisms of intercellular adhesion, cell migration and cancer metastasis [14,24–26]. Considerable effort is focused on understanding the role of biomolecular condensates in functional aspects of cancer pathogenesis, anti-cancer therapeutics, and in immune and antiviral mechanisms in normal and cancer cells [14,24–26]. Remarkably, it is also now recognized that replication of many viruses involves phase-separated liquid droplets [e.g. vesicular stomatitis (VSV), rabies (Negri bodies), influenza A, Ebola, measles, Epstein-Barr, and SARS-CoV-2 viruses][12,14,27,28]. Indeed, MxA condensates sequester viral proteins such as the nucleocapsid protein of different viruses [e.g. the La Crosse (LACV) and VSV][9,12]. However, the significance of condensate formation by Mx proteins in their antiviral activity is incompletely understood.

2. Genetic Susceptibility or Resistance of Mice to Inhaled Influenza A Virus (FLUAV) Challenge

Pioneering work by Lindenmann and colleagues in the 1960s led to the recognition that inbred laboratory stains of Balb/c mice were susceptible to a nasal challenge by influenza A virus (FLUAV)[29]. In contrast, the A2G strain of mice as well as outbred and field mice were resistant to such virus challenge [29]. Subsequently Haller and colleagues recognized that this viral resistance depended on the production of interferon triggered by the virus challenge [30]. Further genetic analyses showed that this IFN-dependent myxovirus resistance of A2G mice and of wild-type mice represented a wild-type genetic trait dubbed $Mx^{+/+}$ while inbred FLUAV susceptible Balb/c mice were homozygous mutants at this locus ($Mx^{-/-}$)[1–3,29,30]. The IFN-induced antiviral gene product involved was eventually identified as a 60-kDa dynamin family GTPase called Mx1 in the mouse, while the corresponding human gene product, initially also called Mx1, was eventually dubbed MxA [1–3]. Both murine Mx1 and human MxA were shown to be antiviral towards diverse RNA- and DNA viruses. Additionally, a second Mx gene product, the murine Mx2 and human MxB was discovered in each species. These too showed antiviral activity but towards a more limited range of viruses [1–3].

To clarify the nomenclature of the Mx protein family [1–4,31]: most mammalian Mx proteins are formed from two distinct gene lineages (*MxA* or *MxB*) that arose from an ancient duplication event. Thus, humans have two Mx proteins – MxA and MxB (some investigators continue to call these proteins as human Mx1 and human Mx2 respectively). Although mice also have two Mx proteins – Mx1 and Mx2, both these are paralogous members of the human MxA lineage. The genuine ortholog of human MxB has been lost in rodent and felid lineages [1–3,31]. Thus, human MxB and murine Mx2 are *not* orthologous. While the major human Mx protein ("MxA") is cytoplasmic, its orthologous major murine Mx protein ("Mx1") is nuclear. Curiously, the less abundant orthologous murine Mx protein ("Mx2") is cytoplasmic. The terms *Mx1* and *Mx2 (in italics)* are used for the respective genes in both human and murine species. In this article we use MxA or HuMxA for the cytoplasmic human protein, and Mx1 or MuMx1 for the orthologous nuclear murine protein. Human MxB is a

Preprints.org (www.preprints.org) | NOT PEER-REVIEWED | Posted: 26 September 2024 doi:10.20944/preprints202409.1952.v

cytoplasmic protein representing the second gene lineage; cytoplasmic murine Mx2 is orthologous to human MxA and not MxB [1–3,31].

Parenthetically, rats have three Mx proteins Mx1, Mx2 and Mx3 [1–4]. Rat Mx1 and rat Mx2 are orthologs of human MxA, and are nuclear and cytoplasmic respectively. However, the nuclear-predominant rat Mx1 has antiviral activity towards both FLUAV and VSV, while the cytoplasmic-predominant rat Mx2 is antiviral towards VSV only [1–4]. Rat Mx3, which is mainly dispersed in the cytoplasm, has little apparent antiviral activity [1–4].

3. Distinct Subcellular Localization of the Major Human and Murine Mx Proteins

Human MxA and its *orthologous* murine Mx1 localize predominantly to *different* cellular compartments. The human protein is cytoplasmic while the orthologous murine protein, which has a weak nuclear-localization signal, is largely, but not exclusively nuclear [30](Figure 1). Human MxA also forms cytoplasmic filaments (Figure 2)[12,14].

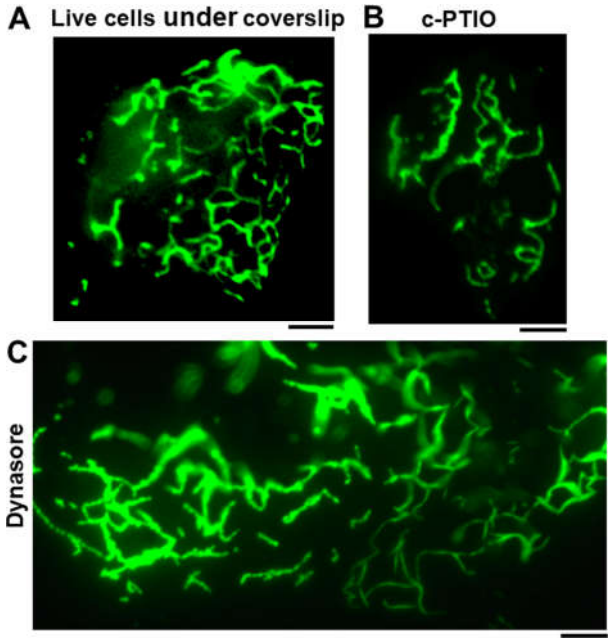

Figure 2. Spheroid to fibril transformation of GFP-MxA condensates in live cells. **(A)** Huh7 cells expressing GFP-MxA as spheroids were placed under coverslip in a drop of PBS and imaged 30 to 40 min later. **(B)** GFP-MxA filaments in Huh7 cells exposed to the nitroc oxide scavenger c-PTIO (100 μM, 7 hr) or (**C)** to dynasore (20 nM, 4 days). All scale bars = 5 μm. By time-lapse imaging, these filaments were mobile in the cytoplasm. From ref. [12]. .

In terms of antiviral activity, briefly, cytoplasmic human MxA is antiviral towards FLUAV and VSV, but nuclear murine Mx1 is antiviral towards FLUAV but not VSV (Table 1)(Figure 3)[12]. More broadly, human MxA is antiviral towards several RNA- and DNA-containing viruses including orthomyxo- and rhabdoviruses [1–4]. The data in Figure 3 show the antiviral activity of human GFP-MxA against VSV in Huh7 cultures at the single- cell level [12]. In many such cells, remnants of the VSV nucleocapsid (N) protein are seen co-associated with GFP-MxA condensates (single white arrows)[12].

Preprints.org (www.preprints.org) | NOT PEER-REVIEWED | Posted: 26 September 2024 doi:10.20944/preprints202409.1952.v

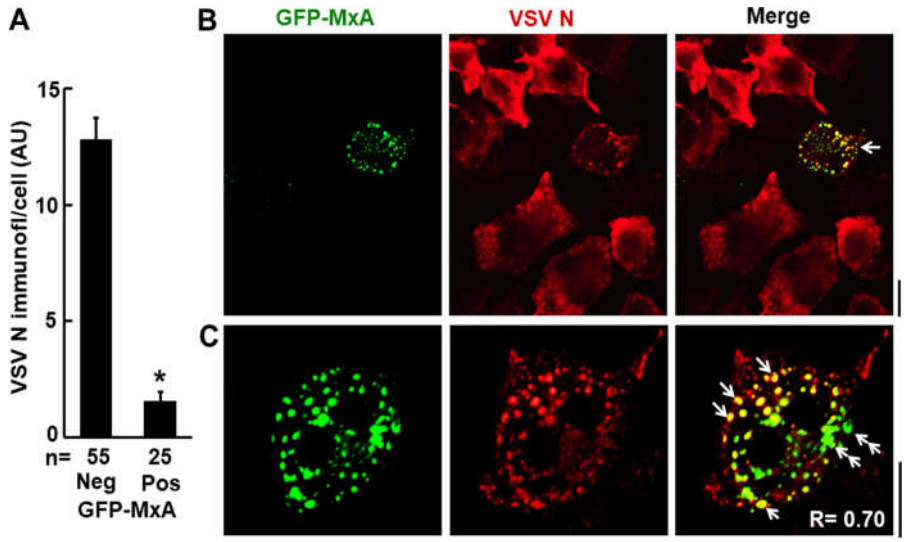

Figure 3. Antiviral activity of exogenously expressed GFP-MxA in Huh7 cells. GFP-MxA expressing cells were infected with VSV Orsay wt at MOI > 10 pfu/cell, fixed 4 hr later and stained for VSV N protein. **(A)** antiviral efficacy. **(B)** representative image fields. **(C)** high magnification images of 1 cell out of 19 such. Single white arrows inclusion of VSV N in spheroidal GFP-MxA condensates, double white arrows, GFP-MxA without N in irregular condensates. Scale bars=20 μm. R = Pearson's coefficient. From Ref. [12].

In addition to formation of nuclear structures by murine GFP-Mx1 (Figure 1), we recently observed that in 20-30% of transfected cells in a human Huh7 hepatoma cell culture, exogenously expressed murine GFP-MuMx1 formed cytoplasmic bodies/condensates and a meshwork of *cytoplasmic* intermediate filaments (Figure 4)[30]. In a novel finding, while cells with GFP-Mx1 only in their nucleus showed no antiviral activity against VSV, cells with cytoplasmic MuMx1 displayed antiviral activity towards VSV (Figure 5, Table 1)[32]. It is long known that FLUAV has cytoplasmic and nuclear steps in its replication cycle, while the VSV replication cycle is completely confined to the cytoplasm [31]. Not surprisingly, murine Mx2, which forms cytoplasmic granules is also antiviral towards VSV [33]. Thus, the subcellular localization of respective Mx protein condensates critically regulates their antiviral phenotype (Table 1) [7,32].

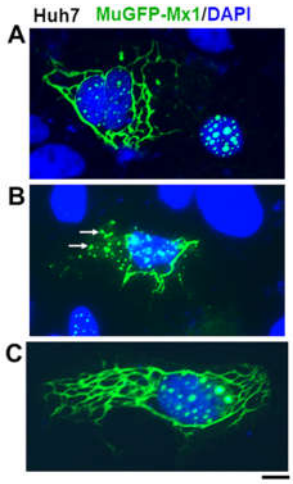

Figure 4. (A, B, C) Cytoplasmic filaments and cytoplasmic bodies (white arrows) of murine GFP-Mx1 in 20-30% of human hepatoma Huh7 hepatoma cells following transient transfection. Cells with nuclear bodies *only* were also observed in the same images as in (A) and Figure 1B. Scale bar = 10 μm. Adapted from ref. [32].

Preprints.org (www.preprints.org) | NOT PEER-REVIEWED | Posted: 26 September 2024 doi:10.20944/preprints202409.1952.v

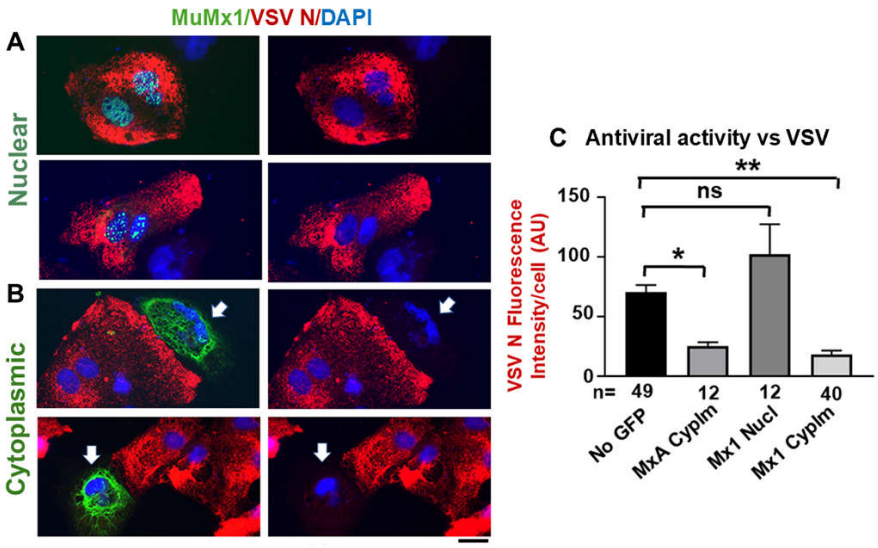

Figure 5. Novel antiviral activity of cytoplasmic murine GFP-Mx1 expressed in human Huh7 cells but not nuclear expressed GFP-Mx1 against VSV. Cultures of Huh7 cells were transiently transfected with expression vectors for GFP-MxA (as positive controls) and GFP-Mx1 **(A)** and **(B)** above were infected with VSV (at moi > 10 pfu/cell). Cultures were fixed 4 hrs later and evaluated for VSV N protein expression (red). White arrows indicate cells expressing murine GFP-Mx1 in the cytoplasm with evidence of an antiviral phenotype. **(C)** Image J was used for quantitating N protein expression in respective cells. By ANOVA: ns, not significant; * $P < 0.01$; ** $P < 0.001$. Scale bar = 10 μm. Adapted from From ref. [32].

Cytoplasmic full-length human MxB, which is mainly associated with the cytoplasmic side of nuclear pores, has antiviral activity against HIV and other lentiviruses, and herpesvirus by blocking entry of viral components into the nucleus [7,16–18](Table 1).

4. Overview of MxA Protein Structure

MxA has an overall structure consisting of a globular GTPase domain (G domain), a hinge region (BSE region), a stalk consisting of 4 extended alpha-helices, connected by four unstructured loops (prominently the L4 loop in the C-terminal half) (Figure 1D, 1B)[1–3,8,34,35]. In the cell cytoplasm, endogenous wild-type MxA as well as exogenously expressed wt MxA form variably shaped and sized structures [1–3,36–38]. MxA dimerization and oligomerization have been studied extensively in cell-free assays [1–3]. The dimerization has been attributed to an interface in the G domain, especially the D250 residue in MxA as well as the stalk region [8,34,35]. The L4 loop (residues 533-572 in HuMxA) is a 40-amino acid long intrinsically disordered region (IDR) which includes a stretch of 4 polylysines (single arrows in Figure 1D, 1E). Human MxB and murine Mx1 both possess IDR regions that approximately correspond to the L4 loop in MxA (Figure 1E). Moschonas et al [18] reported recently that the IDR region in MxB drove the phase-separated biomolecular condensate formation. MxA has an additional IDR containing two vicinal Cys residues (Cys42 and Cys52) located at the N terminus of the protein [14]. Which structural domains of human MxA and murine Mx1 drive phase-separation and condensate formation has not yet been experimentally determined.

The GTPase activity and the L4 IDR loop contribute to the antiviral phenotype [1–4,34,35]. In mutational studies in intact cells, the D250A mutant of MxA which lacks GTPase activity and fails to dimerize, was found to lack antiviral activity and to remain dispersed in the cytoplasm [34,35]. The C-terminal part of the L4 IDR loop (residues 533-572 in MxA) served as a major antiviral determinant. A single amino acid in the L4 loop (F561) of MxA largely determined antiviral activity against orthomyxoviruses [1-4,34,35]. SUMOylation of MxA protected against its degradation and enhanced antiviral potency of MxA against VSV [1–3]. The biochemical basis for how Mx proteins mediate antiviral activity at the molecular level is focused on inhibition of early viral transcription, and this

Preprints.org (www.preprints.org) | NOT PEER-REVIEWED | Posted: 26 September 2024 doi:10.20944/preprints202409.1952.v

activity is attributed to dispersed soluble cytosolic MxA [5,6]. Curiously, GTPase null mutants of MxA, which are devoid of antiviral activity against most viruses can still form large cytoplasmic structures [34,35]. Thus, GTPase activity is not necessary for condensate formation. Our working hypothesis is that MxA condensates represent a storage depot of antivirally active protein, while the antiviral activity *per se* is mediated by dispersed MxA (Figure 6)[36–38].

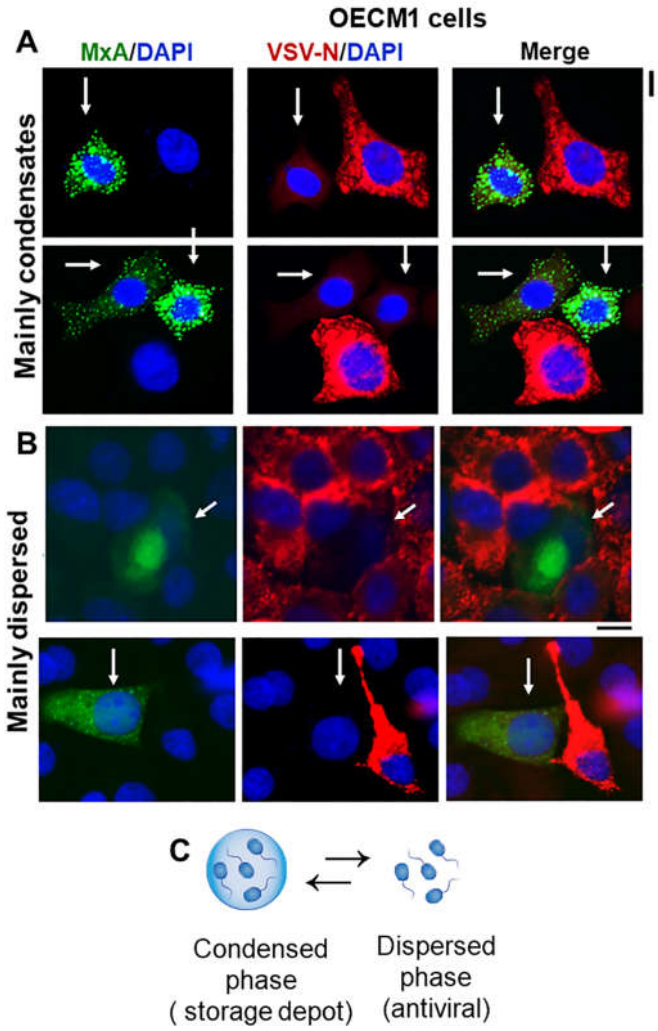

Figure 6. Single-cell antiviral phenotype (protected against VSV; white arrows) of oral carcinoma (OECM1) cells expressing GFP-MxA mainly in condensates **(A)** or mainly in the dispersed phase **(B).** Cultures in 35 mm plates were transiently transfected with pGFP-MxA vector, and two days later were challenged with VSV (moi >10 pfu/cell), and fixed 24 hr after the start of infection [34]. VSV replication was assessed by immunostaining for the VSV nucleocapsid (N) protein (in red)[24,27,29]. White arrows point to GFP-containing cells with reduced VSV-N. Scale bars = 20 μm. **(C)** schematic highlighting the dynamic equilibrium between GFP-MxA in condensed vs dispersed phase. Adapted from ref. [38].

5. Discovery of Cytoplasmic MxA Protein Structures as Membraneless Phase-Separated Biomolecular Condensates

In the last 5 years we recognized that cytoplasmic human MxA structures represented dynamic metastable membraneless liquid-liquid phase-separated (LLPS) biomolecular condensates (Table 1 , Figure 1A, Figure 1C) [12–15,36]. Moreover, nuclear murine Mx1 structures also represented LLPS-driven biomolecular condensates (Figure 1B)[32]. And, more recently cytoplasmic human MxB structures have also shown to be LLPS-driven biomolecular condensates [18].

Preprints.org (www.preprints.org) | NOT PEER-REVIEWED | Posted: 26 September 2024 doi:10.20944/preprints202409.1952.v

To summarize several of the new findings [12–15], we observed using correlated light and electron microscopy methods (CLEM) that GFP-MxA transiently expressed in human cells formed structures in the cytoplasm that were membraneless by thin-section EM (Figure 1C). These spheroidal structures were variably sized, and metastable in that they fused with each other in live-cell time-lapse observations, and even generated filaments upon pressure by a coverslip or exposing cells to dynasore (a GTPase inhibitor) or c-PTIO (a NO scavenger)(Figure 2)[12]. In FRAP assays the GFP-MxA structures had a gel-like internal consistency. Moreover, such structures were disassembled by hypotonicity, and by 1,6-hexanediol (reagents which disrupt phase-separated condensates)[12,37,38]. Importantly, IFN-α and λ-induced *endogenous* MxA also formed structures in the cytoplasm which showed properties of LLPS-driven biomolecular condensates [12,13,37,38]. Similar techniques have been used recently to show that human MxB structures are also LLPS-driven biomolecular condensates [18]. Additionally, murine GFP-Mx1 mainly formed spheroidal phase-separated biomolecular condensates in the nucleus ("nuclear bodies"). In FRAP assays, nuclear Mx1 bodies evidenced a gel-like interior. Hypotonicity and 1,6-hexanediol also disassembled murine Mx1 bodies [32]. The realization that human and murine Mx structures in the cytoplasm and nucleus represent LLPS-driven biomolecular condensates forming "membraneless organelles" (MLOs) represents a major paradigm shift in this field of virology.

6. Rapid Reversible Metastability of MxA Condensates in Cancer Cells

In many of our recent experiments we have focused on studies of the rapid dynamic changes of human MxA condensates in cancer cells – liver, lung, melanoma and oral carcinoma cells (Figure 7A). A more recent focus has been to investigate the rapid dynamic regulation of MxA condensates at a major portal for the entry of myriad viruses into the body -- in oral epithelial cells subjected to environmental stresses [such as of hypotonicity (water, tea and coffee), hypertonicity (wine and juices), and of temperature (cold and warm drinks)] routinely inflicted upon the oral mucosa [38]. We note that it was already reported in 2012 that MxA was constitutively expressed in healthy periodontal tissues, and that this expression was decreased in patients with periodontitis [39]. MxA expression in oral/gingival epithelial cells in culture was upregulated by IFN-λ1 and α-defensins, two cytokines constitutively present in the gingival mucosa [38,39]. We note that normal saliva is normally hypotonic – it has one-third tonicity (approx. 100 mOsm) compared to plasma (approx. 285-330 mOsm)(reviewed in [38]). Thus, oral mucosal cells – a site for replication of many incoming viruses - are always under hypotonic stress conditions.

We observed in a variety of cell types (human liver, lung, melanoma and oral carcinoma cells) that MxA condensates were exquisitely sensitive, rapid and reversible sensors of hypotonicity (Figure 7A)[12,32,37]. In cells kept in normal culture medium (approx. 300 mOsm) approximately 80-90% of cytoplasmic MxA was observed in the dense or condensed phase. This dropped to less than 10% of MxA in the dense state within 2-3 min of transfer of all cell types tested to one-third, or one-tenth hypotonicity medium (Figure 8)[12]. Following exposure of cells to one-tenth tonicty (and thus complete disassembly of MxA condensates in 1-3 minutes), the subsequent shifting of cells to isotonicity led to rapid reassembly of new condensates within 20-60 seconds (Figure 7A) [12]. We have carried out up to three cycles of disassembly and reassembly in time-lapse studies of the same culture (adjusting tonicity with sucrose) (Figure 7A)[12]. Impressively, even the continued maintenance of lung and oral carcinoma cells in say one-third or one-fourth tonicity medium (similar to saliva), led to a spontaneous reassembly of the previously disassembled MxA into new MxA condensates within 5-7 min (Figure 8)[37,38].

Preprints.org (www.preprints.org) | NOT PEER-REVIEWED | Posted: 26 September 2024 doi:10.20944/preprints202409.1952.v

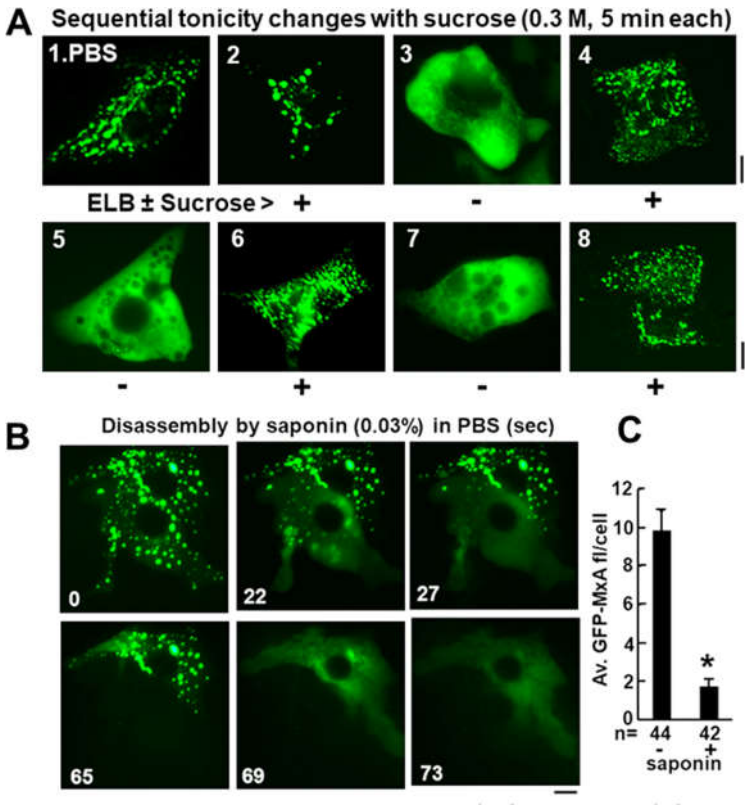

Figure 7. (A) Dissecting the mechanism of hypotonic disassembly and isotonic reassembly of GFP-MxA condensates. A culture of Huh7 cells expressing GFP-MxA kept continuously at 37°C was sequentially imaged in 5-min steps in the indicated media [isotonic PBS (300 mOsm), hypotonic ELB (40 mOsm), or ELB+sucrose (330 mOsm)]. **(B)** Huh7 cells kept in PBS expressing GFP-MxA condensates were imaged just before and just after exposure to saponin (0.03%) in a time-lapse series (in seconds). **(C)** Quantitation of the loss of GFP-MxA from saponin-treated cells (within 2 to 5 min). *, $P < 0.001$. Adapted from ref. [12].

Most cells tested, especially lung A549 adenocarcinoma and oral OECM1 carcinoma cells, contained cellular and biochemical mechanisms that mediate regulatory volume decrease (RVD) that partition back most cytoplasmic MxA into the condensed phase. We suspect that these mechanisms include (a) internalization of excess plasma membrane of swollen cells into intracellular vacuole-like dilations (VLDs) compressing the cytosol; (b) the hypotonicity-driven water influx, and then water efflux during recovery-phase RVD driven by the WNK-SPAK/OSR1-PTP-KCC pathway [the "With-no-Lysine kinase-Ste20-type kinases-protein phosphatase- K-Cl cotransporter" pathway]; and (c) the biophysical uncrowding and recrowding of cytosolic contents as water enters and leaves the cell {Figure 9). Specifically, oral carcinoma cells (OECM1) preloaded with calcein-AM when exposed to hypotonicity showed an increase in fluorescence corresponding to unquenching/molecular uncrowding of cytosol concomitant with GFP-MxA disassembly [38]. A subsequent de crease in calcein-AM fluorescence corresponding to requenching/recrowding of cytosol accompanied reformation of GFP-MxA condensates [38]. These data suggested an initial influx of water followed by an efflux. Thus, the partitioning of MxA into the dense condensate vs dispersed phases is exquisitely regulated by intracellular water.

Preprints.org (www.preprints.org) | NOT PEER-REVIEWED | Posted: 26 September 2024 doi:10.20944/preprints202409.1952.v

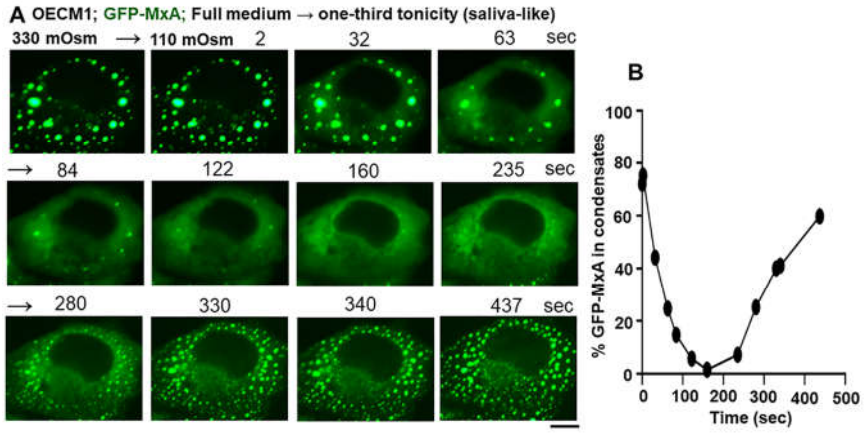

Figure 8. Spontaneously reversible osmosensing by GFP-MxA condensates in oral epithelial cells - focus on saliva-like hypotonicity. **(A)** Sequential live-cell imaging of the same OECM1 cell expressing GFP-MxA condensates 2 days after transient transfection first in full culture medium (330 mOsm) and then after shifting to hypotonic of one-third tonicity (110 mOsm; full medium diluted 1:2 with water) for the next 8-10 min to match saliva hypotonicity. Scale bar = 10 µm. **(B)** Quantitation of GFP-MxA in condensates on a % per cell basis in the images shown in **(A).** This quantitation was carried out using the small object subtract Filter in Image J. From ref. [38]. .

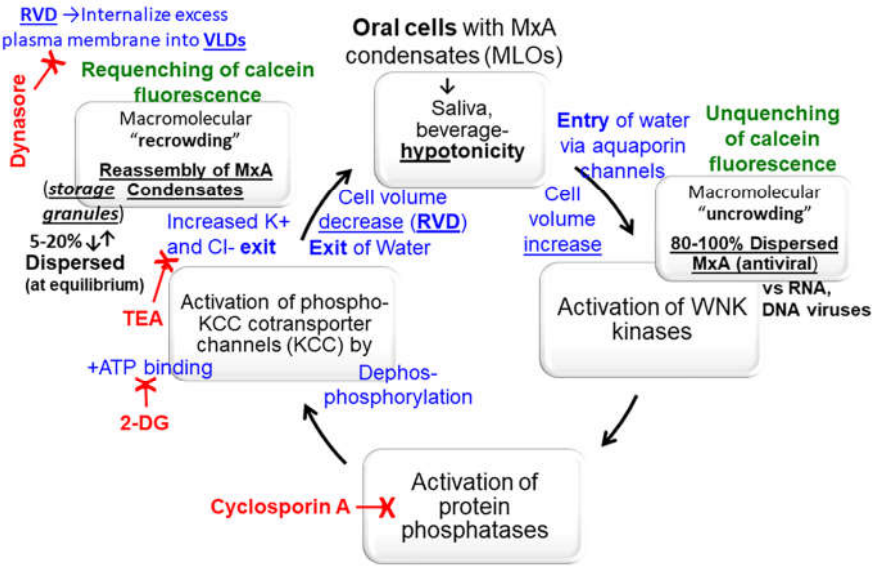

Figure 9. Overview of the biophysical and biochemical mechanisms possibly involved in the cell-volume driven dynamic regulation of the formation, disassembly and reassembly of MxA condensates in oral epithelial cells subjected to saliva- and beverage-like hypotonicity. 2-DG, 2-deoxyglucose; KCC, potassium-chloride cotransporter channels 1-4; MLO, membraneless organelle, TEA, tetraethylammonium chloride; RVD, regulated volume decrease; VLD, vacuole-like dilatations; WNK kinase, "With no lysine" kinase family members 1-4. Adapted from ref. [38].

In terms of antiviral activity, cells with MxA mainly in the condensate phase or mainly in the dispersed phase both showed equivalent antiviral phenotype at least against VSV (Figure 6)[38]. This led to the hypothesis that condensates might represent a storage form of MxA while the antiviral activity resided in MxA in the dispersed phase (as was proposed in 1999 by Pavlovic and colleagues;[8]). Hypotonicity-driven disassembly and isotonicity-driven reassembly were also observed for the *nuclear* murine Mx1 condensates, suggesting that intracellular changes in water content permeated both the cytoplasmic and nuclear compartments [32].

Preprints.org (www.preprints.org) | NOT PEER-REVIEWED | Posted: 26 September 2024 doi:10.20944/preprints202409.1952.v

7. Additional Aspects of Metastability Include the Following

7.1. HA or GFP Tags Affect Appearance of MxA Condensates in the Cytoplasm

Exogenously expressed HA-tagged MxA or GFP-tagged MxA formed cytoplasmic condensates with a perceptible difference in their fine structure. In addition to discrete variably-sized cytoplasmic structures, HA-MxA in Huh7 hepatoma cells often draped along the giantin-based intermediate filament meshwork contained in these cells giving rise to a meshwork appearance [12,14]. In contrast GFP-MxA structures remained spheroidal, even when lying alongside intermediate filaments. IFN-induced endogenous MxA in various cell types mainly formed discrete variably-sized, spheroidal as well as variably-shaped structures [12,14].

7.2. Integrity of MxA Condensates Requires Intact Cells

Exposure of Huh7 cells containing GFP-MxA condensates to low concentrations of nonionic detergent such as 0.03% saponin, which pokes holes in the plasma membrane, led to the disassembly of condensates within 15-60 seconds with visible leakage of the GFP into the culture medium (Figure 7B)[12]. For most condensates in many cells, this disassembly was complete. However, a subset of GFP-MxA condensates in some cells showed a detergent-resistant core [12]. Data from proteomics studies of GFP-MxA condensates as well as those formed by native endogenous MxA in IFN-treated cells are awaited.

7.3. Spheroid to Fibril Transition

Cytolasmic GFP-MxA condensates in Huh7, A549 and OECM1 cells were mainly variably-sized spheroids which moved around, fused and reassumed a spheroidal shape. However, placement of a coverslip on live Huh7 cells elicited a transition of GFP-MxA to fibrils (we suspect this to result from mechanical pressure and hypoxia)(Figure 2)[12]. Also, exposure of cells to a GTPase inhibitor (dynasore) or nitric oxide scavenger (c-PTIO) led to a spheroid to fibril transition (Figure 2)[12]. By time-lapse imaging these filaments waved around in the cytoplasm. The biochemical bases of this transition to fibrils and its biological consequences are not understood.

7.4. Incomplete Mixing of Proteins within GFP-MxA Condensates

GFP-MxA expressing Huh7 cells were largely resistant to infection by VSV in single-cycle infection experiments using an moi > 10 pfu/cell as judged by immunofluorescence assays of the VSV nucleocapsid (N) protein at the single-cell level (Figure 3)[12]. In a subset of infected and GFP-MxA expressing cells, the VSV N protein was observed to associate with spheroidal MxA condensates with the N and GFP fully overlapping (Figure 3, single white arrows). Interestingly, the variably distorted GFP-MxA condensates in the same cells showed only a partial overlap with N (Figure 3, double white arrows). Thus, these condensates provided evidence of incomplete mixing of protein components. We note that FRAP data showed only a gel-like consistency within GFP-MxA condensates and not free mixing [12].

8. Conclusions

Studies of the antiviral human and murine Mx proteins as biomolecular condensates are in their initial stages. Nevertheless, sufficient information is already available to demonstrate exciting new aspects of the dynamic regulation of Mx condensates by intracellular water. The exquisitely sensitive and rapid osmosensing by human MxA condensates in oral cancer cells to hypotonicity mimicking saliva-like conditions is remarkable. The detailed regulatory biochemistry of MxA condensates in the response of such cells to environmental stresses of ingesting different liquids may well emulate the regulation of water and salt influx and efflux already worked out for different cells in different portions of the renal tubules (e.g. the WNK-SPAK/OSR1-PTP-KCC pathway; [38]). We are excited by the prospect of elucidating this biochemistry as it pertains to MxA condensates and antiviral mechanisms that are likely to be part of barrier immunity in the mouth. Overall, studies of

Preprints.org (www.preprints.org) | NOT PEER-REVIEWED | Posted: 26 September 2024 doi:10.20944/preprints202409.1952.v

biomolecular condensates of different antiviral Mx proteins in the cytoplasmic and nuclear compartments in different species (human and murine) are a work in progress.

Funding: This research received no external funding.

Data Availability Statement: All data are available within this manuscript.

Conflicts of Interest: The author declares no conflicts of interest.

References

1. Haller, O. and Kochs, G. (2002). Interferon-induced mx proteins: dynamin-like GTPases with antiviral activity. *Traffic* **3,** 710-717.
2. Haller, O., Staeheli, P., Kochs, G. (2007) Interferon-induced Mx proteins in antiviral host defense. *Biochimie* **89,** 812-818.
3. Haller, O., Staeheli, P., Schwemmle, M. and Kochs, G. (2015) Mx GTPases: dynamin- like antiviral machines of innate immunity. *Trends Microbiol* **23, 1**54-163.
4. Verhelst, J., Hulpiau, P. and Saelens, X. (2013) Mx proteins: antiviral gatekeepers that restrain the uninvited. *Microbiol. Mol. Biol. Rev.* **77,** 551-566.
5. Staeheli, P., Pavlovic, J. (1991) Inhibition of vesicular stomatitis virus mRNA synthesis by human MxA protein. *J Virol* **65,** 4498-4501.
6. Schwemmle, M.,Weining, K.C., Richter, M.F., Shumacher B., Staeheli, P. (1996) Vesicular stomatitis virus transcription inhibited by purified MxA protein. *Virology* **206,** 545-554.
7. Steiner, F., Pavlovic, J. (2020) Subcellular localization of MxB determines its antiviral potential against influenza virus. *J Virol* **94,** e00125-e220
8. DiPaolo, C., Hefti, H. P., Meli, M., Landis, H., and Pavlovic, J. (1999) Intramolecular backfolding of the carboxyl-terminal end of MxA protein is a prerequisite for its oligomerization. *J Biol Chem* **274,** 32071-32078.
9. Kochs, G., Janzen, C., Hohenberg, H., Haller, O. (2002) Antivirally active MxA protein sequesters La Crosse virus nucleocapsid protein into perinuclear complexes. *Proc Natl Acad Sci USA* **99,** 3153-3158.
10. Accola, M. A., Huang, B., Al Masri, A. and McNiven, M. A. (2002). The antiviral dynamin family member, MxA, tubulates lipids and localizes to the smooth endoplasmic reticulum. *J. Biol. Chem.* **277,** 21829-21835.
11. Stertz, S., Reichelt, M., Krijnse-Locker, J., Mackenzie, J., Simpson, J. C., Haller, O. and Kochs, G. (2006). Interferon-induced, antiviral human MxA protein localizes to a distinct subcompartment of the smooth endoplasmic reticulum. *J. Interferon Cytokine Res.* **26,** 650-660.
12. Davis, D., Yuan, H., Liang, F.X., Yang, Y.M., Westley, J., Petzold, C., Dancel-Manning, K., Deng, Y., Sall, J. and Sehgal, P.B. (2019) Human antiviral protein MxA forms novel metastable membraneless cytoplasmic condensates exhibiting rapid reversible tonicity- driven phase transitions. *J Virol* **93,** e01014-19.
13. Davis, D., Yuan, H., Liang, F.X., Sehgal, P.B. (2018) Interferon-α-induced cytoplasmic MxA structures in hepatoma Huh7 and primary endothelial cells. *Contemp Oncology (Pozn)* **22,** 86-94.
14. Sehgal, P. B., Westley, J., Lerea, K. M. DiSenso-Browne, S. and Etlinger, J. D. (2020) Biomolecular condensates in cell biology and virology: phase-separated membraneless organelles (MLOs). *Analytical Biochem* **597**, 113691.
15. Sehgal, P. B. and Lerea, K. L. (2020) Biomolecular condensates and membraneless organelles (MLOs). In Jez. Joseph (Eds) *Encyclopedia of Biological Chemistry*, 3rd Edn., vol. 1, pp 530-541. Oxford: Elsevier. https://doi.org/10.1016/B978-0-12-819460-7.00003-7
16. Goujon, C., Mancorge, O., Bauby, H., Doyle, T., Barclay, W.S., Malim, M.H. (2014) Transfer of the amino-terminal nuclear envelope targeting domain of human MX2 converts MX1 into an HIV-1 resistance factor. *J Virol* **88,** 9017-9026.
17. Dicks, M.D.J., Betancor, G., Jimenez-Guardeno, J.M., Pessel-Vivares, L., Apolonia, I., Goujon, C., Malim, M.H. (2018) Multiple components of the nuclear pore complex onteract with the amino terminus of MX2 to facilitate HIV-1 restriction. *PLoS Pathog* **14,** e1007408
18. Moschonas, G. D., Delhaye, L., Cooreman, R., Bhat, A., Sutter, D. D., Parthoens, E., Desmer, A, Maciejczak, A, Grzek, H., Lippens, S., Debyser, Z., Eyckerman, S., Saelens, X. (2023) MX2 restricts HIV-1 and herpes simplex virus-1 by forming cytoplasmic biomolecular condensates that mimic nuclear pore complexes. bioArxiv preprint doi: https://doi.org/10.1101/2023.06.22.545931

Preprints.org (www.preprints.org) | NOT PEER-REVIEWED | Posted: 26 September 2024 doi:10.20944/preprints202409.1952.v

19. Banani, S.F., Lee, H.O., Hyman, A.A. and Rosen, M.K. (2017) Biomolecular condensates: organizers of cellular biochemistry. *Nat Rev Mol Cell Biol.* **18,** 285-298.
20. Shin, Y. and Brangwynne, C.P. (2017) Liquid phase condensation in cell physiology and disease. *Science* **357**(6357) pii: eaaf4382. doi: 10.1126/science.aaf4382.
21. Alberti, S. (2017) The wisdom of crowds: regulating cell function through condensed states of living matter. *J Cell Sci.* **130,** 2789-2796.
22. Alberti, S., Gladfelter, A. and Mittag, T. (2019) Considerations and challenges in studying liquid-liquid phase separation and biomolecular condensates. Cell **176,** 419-434.
23. Shin, Y., Berry, J., Pannucci, N., Haataja, N. P. Toettcher, J. E. and Brangwynne, C. P. (2017) Spatiotemporal control of intracellular phase transitions using light-activated optoDroplets. *Cell* **168,** 159-171.
24. Boija, A., Klein, I.A., Young, R.A. (2021) Biomolecular condensates and cancer. *Cancer Cell* **39,** 174-192.
25. Banerjee, P.R., Holehouse, A.S., Kriwacki, R., Robustelli, P., Jiang, H., Sobolevsky, A.I., Hurley, J.M., Mendell, J.T. (2024) Dissecting the biophysics and biology of intrinsically disordered proteins. *Trends Biochem Sci* **49,** 101-104.
26. Shimeki, H.K., Chandra, B., Kriwacki, R.W. (2023) Dissolving fusion oncoprotein condensates to reverse aberrant gene expression. *Cancer Res* **83,** 3324-3326.
27. Heinrich, B.S., Maliga, Z., Stein, D.A., Hyman, A.A. and Whelan, S.P.J. (2018) Phase transitions drive the formation of vesicular stomatitis virus replication compartments. *MBio* **9,** e02290-17. doi: 10.1128/mBio.02290-17.
28. Carlson, C. R., J.B. Asfaha, C.M. Ghent, C.J. Howard, N. Hartooni, D.O. Morgan (2020) Phosphoregulation of phase separation by the SARS-CoV-2 N protein suggests a biophysical basis for its dual functions. *Mol Cell* **80,** 1092-1103.e4
29. Lindenmann, J., Lane, C.A., Hobson, D. (1963) The resistance of A2G mice to myxoviruses. *J Immunol* **90,** 942-951.
30. Haller, O., Arnheiter, H., Gresser, I., Lindenmann, J. (1979) Genetically determined, interferon-dependent resistance to influenza virus in mice. *J Exp Med* **149,** 601-612.
31. Bunasdiego, I., Kane, M., Rihn, S.J., Preugschas, H.F., Hugher, J., Blanco-Melo, D., Strouvelle, V.P., Zang, T.M., Willet, B.J., Boutell, C., Bienlasz, P.D., Wilson, S.J. (2014) Host and viral determinants of Mx2 antiretroviral activity. *J Virol* **88,** 7738-7752**.**
32. Sehgal, P. B., Yuan, H., Scott, M. F., Deng, Y., Liang, F-X. and Mackiewicz, A. (2020) Murine GFP-Mx1 forms phase-separated nuclear condensates and associates with cytoplasmic intermediate filaments: novel antiviral activity against vesicular stomatitis virus. *J Biol Chem* **294,** 15218-15234
33. Jin, H.K., Takada, A., Kon, Y., Haller, O., Watanabe, T. (1999) Identification of the murine *Mx2* gene: interferon-induced expression of Mx2 protein from feral mouse gene confers resistance to vesicular stomatitis virus. *J Virol* **73,** 4925-4930.
34. Dick, A., Graf, L., Olal, D., von der Malsburg, A., Gao, S., Kochs, G. and Daumke, O. (2015) Role of nucleotide binding and GTPase domain dimerization in dynamin-like myxovirus resistance protein A for GTPase activation and antiviral activity. *J Biol Chem* **290,** 12779–12792.
35. von der Malsburg, A., Abutbul-Ionita, I., Haller, O., Kochs, G. and Danino, D. (2011) Stalk domain of the dynamin-like MxA GTPase protein mediates membrane binding and liposome tubulation via the unstructured L4 loop. *J Biol Chem* **286,** 37858–37865.
36. Sehgal, P. B. (2021) Metastable biomolecular condensates of interferon-inducible antiviral Mx-family GTPases: a paradigm shift in the last three years. *J Biosci* **46,** 72. Doi: 10.1007/s12038-021-00187-x
37. Sehgal, P.B., Yuan, H., Jin, Y. (2022) Rapid reversible osmoregulation of cytoplasmic biomolecular condensates of human interferon-α-induced antiviral MxA GTPase. *Intl J Mol Sci* **23,** 12739.
38. Sehgal, P.B., Yuan, H., Centone, A., DiSenso-Browne, S. V. (2024) Oral antiviral defense: saliva- and beverage-like hypotonicity dynamically regulate formation of membraneless biomolecular condensates of antiviral human MxA in oral epithelial cells. *Cells* **13,** 590.
39. Mahanonda, R., Sa-Ard-Iam, N., Rerkyen, P., Thitithanyanoni, A., Subbalekha, K., Pichyangkul, S. (2012) MxA expression induced by α-defensin in healthy human periodontal tissue. *Eur J Immunol* **42,** 946-956.

Disclaimer/Publisher's Note: The statements, opinions and data contained in all publications are solely those of the individual author(s) and contributor(s) and not of MDPI and/or the editor(s). MDPI and/or the editor(s) disclaim responsibility for any injury to people or property resulting from any ideas, methods, instructions or products referred to in the content.